



A contraction model for the flattening and equatorial ridge of Iapetus

David Sandwell^a, Gerald Schubert^{b,*}

^a*Scripps Institution of Oceanography, University of California, San Diego, La Jolla, CA 92037, United States*

^b*Department of Earth and Space Sciences and Institute of Geophysics and Planetary Physics, University of California, Los Angeles, CA 90095-1567, United States*

ARTICLE INFO

Article history:

Received 31 August 2009

Revised 17 June 2010

Accepted 18 June 2010

Available online 25 June 2010

Keywords:

Iapetus

Satellites, Formation

Satellites, Shapes

ABSTRACT

Others have explained the excess flattening of Iapetus by a model in which the moon formed at a high spin rate, achieved isostatic equilibrium by very rapid interior heating caused by short-lived radioactive isotopes (SLRI), and subsequently cooled, locking in the excess flattening with respect to an equilibrium shape at its present spin rate. Here we propose an alternate model that does not require an unusually high initial spin rate or the SLRI. The initial formation of Iapetus results in a slightly oblate spheroid with porosity >10%. Radioactive heating by long-lived isotopes warms the interior to about 200 K, at which point it becomes ductile and the interior compacts by 10%, while the 120 km-thick exterior shell remains strong. The shell must deform to match the reduced volume of the ductile interior, and we propose that this deformation occurs along the equator, perhaps focused by a thinner equatorial shell. The final shape of the collapsed sphere matches the observed shape of Iapetus today, described as an oblate ellipse, except along the equator where strain concentration forms a broad ridge. To maintain this non-equilibrium shape, the thickness of the shell must exceed 120 km. Testing the equatorial focusing hypothesis will require a model that includes non-linear processes to account for the finite yield strength of the thick lithosphere. Nevertheless, we show that the stress in the lithosphere generated by the contraction of the interior is about 3 times greater than the stress needed to deform the lithosphere, so some type of lithospheric deformation is expected.

© 2010 Elsevier Inc. All rights reserved.

1. Introduction

Iapetus stands apart from Saturn's other mid-size icy satellites and even from all the icy moons of the Solar System because of its unusual shape and prominent equatorial ridge (Porco et al., 2005; Thomas et al., 2007). While Iapetus has other unusual properties, it has a hemispheric albedo dichotomy, a dark leading (in its orbit) hemisphere and a bright trailing hemisphere (Cruikshank et al., 1983), it is the farthest of the regular satellites from Saturn, it has a smaller density and smaller silicate mass fraction than all of the mid-size saturnian satellites save for Tethys, we focus here on explaining its shape and its equatorial ridge.

The global shape of Iapetus has been described as that of an oblate spheroid $a - c = 35.0 \pm 3.7$ km (a is the equatorial radius, and c is the polar radius) (Thomas et al., 2007). The shape has been interpreted as the fossil bulge of a constant density body in hydrostatic equilibrium rotating with a period of about 16 h; the present rotation period of Iapetus is about 79 days (Castillo-Rogez et al., 2007; Thomas et al., 2007; Matson et al., 2009). The formation of an equatorial bulge by despinning requires a much higher initial rotation rate having a period of ~ 7 h (Castillo-Rogez et al., 2007), which is

close to the Roche limit spin rate of 3.8 h. If the equatorial bulge of Iapetus is indeed a fossil remnant of a rapidly spinning body, then the despinning of Iapetus to its present rotation rate places a strong constraint on the satellite's thermal and dynamical evolution; the constraint is so strong that thermal modeling places the formation time of Iapetus at between 3.4 and 5.4 Myr after formation of the calcium-aluminum inclusions found in meteorites (Castillo-Rogez et al., 2007; Matson et al., 2009). We present an alternative hypothesis to explain the global shape of Iapetus that does not involve the despinning of the satellite from a rapidly rotating early state of ~ 7 h. In our model the initial spin rate could be 16 h or longer. We attribute the global oblate shape of Iapetus not to the fossil shape of a rapidly spinning body but to the buckling failure of the moon's lithosphere brought about by the shrinkage of the satellite upon loss of interior porosity.

The equatorial ridge on Iapetus extends over more than half of the equator. In cross section, the ridge is approximately triangular in shape with a base of O(200 km) and a height of about 20 km (Denk et al., 2008). The ridge sits atop the global flattening of Iapetus described above. The ridge has been attributed to despinning (Porco et al., 2005; Castillo-Rogez et al., 2007), tectonic upwarping of the surface (Giese et al., 2008), collapse of a ring orbiting Iapetus (Ip, 2006), convection inside Iapetus (Czechowski and Leliwa-Kopystyński, 2008; Roberts and Nimmo, 2009), and dike emplace-

* Corresponding author.

E-mail address: schubert@ucla.edu (G. Schubert).

ment (Melosh and Nimmo, 2009). In our model, the ridge is produced by the rearrangement of material accompanying the buckling failure of the lithosphere that is focused at the equator.

2. Scenario for buckling the lithosphere of Iapetus

We propose that both the oblate shape of Iapetus and its equatorial ridge are caused by shrinkage of the ductile interior after a lithosphere (shell) has formed (Fig. 1). The initial porosity of the interior of Iapetus could have been 10% or even more (Castillo-Rogez et al., 2007). After about 200 Myr, the interior temperature of Iapetus will have reached about 200 K, as shown by the detailed models of Castillo-Rogez et al. (2007). The interior becomes ductile, and the ice compacts by 10%. This will cause the lithosphere to go into compression. The questions are: (1) Is the compressional force large enough to buckle the shell? (2) What is the primary mode of buckling? and (3) What is the final shape of Iapetus? We assume that the rotation (16 h to 79 d rate) of Iapetus causes a small equatorial bulge. This produces an axisymmetric body that provides the initial shape perturbation for the buckling. A second way to focus the buckling at the equator is to have a shell that is about 2 times thinner at the equator than at the poles as proposed by Beuthe (2009).

2.1. Force due to interior contraction

Suppose the ductile interior of Iapetus shrinks by 10% while the outer lithospheric shell remains at its constant initial radius minus some small elastic shrinkage. Removal of the vertical pressure at the base of the shell will produce a large differential stress in the interior of the shell. This stress, integrated over the thickness of the shell h , is the end load available to deform the thin shell. To make this calculation simple, we assume a constant density for Iapetus and calculate mass $M(r)$, gravity $g(r)$, pressure $P(r)$, and integrated end load F .

$$M(r) = \frac{4}{3} \pi r^3 \rho_0 \quad (1)$$

$$g(r) = \frac{GM(r)}{r^2} = \frac{4}{3} \pi G r \rho_0 \quad (2)$$

$$\frac{dP}{dr} = -g(r) \rho_0 \quad (3)$$

$$P(r) = \int_0^r \frac{dP}{dr} dr + P_0 \quad \text{and} \quad P(R) = 0 \quad (4)$$

After integration we find the familiar result

$$P(r) = \frac{2}{3} \pi G \rho_0^2 R^2 \left(1 - \frac{r^2}{R^2}\right) \quad (5)$$

Suppose the interior shrinks so the normal stress on the base of the shell is zero; then the horizontal stress will be approximately equal to this pressure. The end load in units of force per length is the integral of this stress through the thickness of the shell.

$$F = \int_{R-h}^R P(r) dr = \frac{2}{3} \pi G \rho_0^2 \left(h^2 R - \frac{h^3}{3} \right) \quad (6)$$

For a 120 km-thick shell, the end load is $1.4 \times 10^{12} \text{ N m}^{-1}$, which corresponds to a depth-averaged stress of 12 MPa.

2.2. Primary mode of buckling and the requirement of inelastic deformation

Could this end load be large enough to buckle the strong outer shell of Iapetus? Before going into the calculation for buckling of a spherical shell subject to a uniform end load, we'll investigate the flat-Earth buckling problem. The analysis of the folding of the oceanic lithosphere in the Indian Ocean clearly shows that the elastic buckling model needs to be modified to include the finite yield strength of the lithosphere because the elastic buckling stresses are 8 times greater than the integrated yield strength of the plate (McAdoo and Sandwell, 1985). A summary of that analysis follows.

The differential equation describing the flexure w of a thin elastic plate subjected to a uniform end load F and a point vertical load q_0 is given by

$$D \nabla^2 [\nabla^2 w(\mathbf{x})] + F \nabla^2 w(\mathbf{x}) + \Delta \rho g w(\mathbf{x}) = q_0 \delta(\mathbf{x}) \quad (7)$$

where $\nabla^2 = (\partial^2/\partial x^2) + (\partial^2/\partial y^2)$ is the horizontal Laplacian operator, $\Delta \rho$ is the density contrast across the surface of the plate, g is the acceleration of gravity, and D is the flexural rigidity given by

$$D = \frac{Eh^3}{12(1-\nu^2)} \quad (8)$$

where E is Young's modulus and ν is Poisson's ratio. After taking the 2D Fourier transform of this equation, we find

$$D(2\pi k)^4 W - F(2\pi k)^2 W + \Delta \rho g W = q_0 \quad (9)$$

where k is the wavenumber (1/wavelength). The flexure of the plate depends on the strength of the vertical load as well as the end load

$$W(k) = q_0 [D(2\pi k)^4 - F(2\pi k)^2 + \Delta \rho g]^{-1} \quad (10)$$

The deformations become unbounded when the denominator of this equation goes to zero. This buckling behavior occurs at a critical end load given by

$$F_c = (4D\Delta \rho g)^{1/2} \quad (11)$$

and excites a particular wavelength

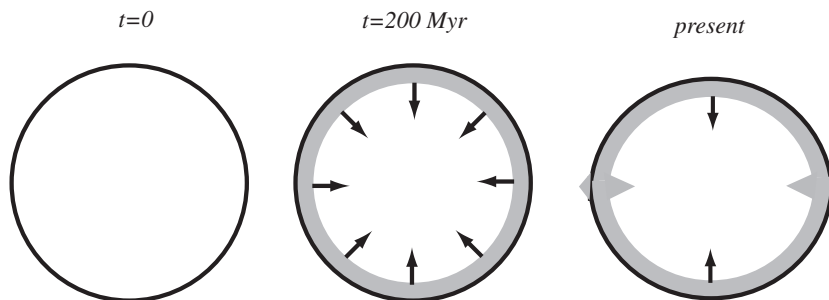


Fig. 1. Diagram showing the gravitational collapse of Iapetus. At time zero the body accretes at an initial radius of r_0 and an average porosity of 10%. After 200 Myr of internal heating, the interior becomes ductile and the porosity decreases to near zero, causing a decrease in volume of the deformable core. Most of the deformation of the thick outer shell occurs near the equator resulting in a N–S collapse of the hemispheres. To conserve the crosssectional area of the shell of the collapsed zone, the inward deformation forming the root of the ridge must have 5 times the crosssectional area of the deformation forming the roof of the ridge. This 5–1 ratio also provides isostatic support for the ridge if the root retains some porosity.

$$\lambda_c = 2\pi \left(\frac{D}{\Delta\rho g} \right)^{1/4} \quad (12)$$

Implementation of this formulation for the Earth results in an unrealistically large critical end load for a typical elastic plate thickness. Since the load exceeds the integrated plate strength F_s by an order of magnitude, McAdoo and Sandwell (1985) proposed a modification to this analysis where the effective plate thickness is reduced as the end load is increased. This happens because brittle deformation near the surface and ductile flow at depth shrink the thickness of the elastic core (McNutt and Menard, 1982). Using a triangular-shaped yield strength envelope, McAdoo and Sandwell (1985) arrived at an effective thickness given by

$$h' = h \left(1 - \frac{F}{F_s} \right)^{1/2} \quad (13)$$

The new critical end load and buckling wavelength are given by

$$F'_c = (4D\Delta\rho g)^{1/2} \left(1 - \frac{F'_c}{F_s} \right)^{3/4} \quad \text{and} \quad \lambda'_c = 2\pi \left(\frac{D}{\Delta\rho g} \right)^{1/4} \left(1 - \frac{F'_c}{F_s} \right)^{3/8}$$

respectively.

The conclusion for the buckling or folding of the oceanic lithosphere on the Earth is that the end load required for elastic buckling is about 10 times greater than the tectonic end load, which is slightly greater than the integrated strength of the plate. We expect a similar behavior on Iapetus, although in this case the “tectonic” end load is known from the gravitational contraction force.

Because the thickness of the lithosphere on Iapetus is not significantly less than the radius of the body, we perform the same buckling analysis using the flexure equations developed by Beuthe (2008). We assume from the outset that the buckling modes are axisymmetric and that the initial perturbation is the ellipsoidal shape of Iapetus caused by rotational flattening. The differential equation for flexure on a sphere is

$$\eta D \nabla^2 \nabla^{2'} \nabla^{2''} w + FR^2 \nabla^{2'} \nabla^{2''} w + EhR^2 \nabla^{2''} w + R^4 (\nabla^2 + 1 - \nu) \Delta\rho g w = R^4 (\nabla^2 + 1 - \nu) q_o \delta(\theta) \quad (14)$$

where

$$\eta = \frac{12R^2}{12R^2 + h^2} \quad (15)$$

and the differential operators are given by

$$\nabla^2 a = \frac{1}{\sin\theta} \frac{\partial}{\partial\theta} \left(\sin\theta \frac{\partial a}{\partial\theta} \right), \quad \nabla^{2'} a = \nabla^2 a + 2a \quad (16)$$

where θ is colatitude. The flexure equations provided in Beuthe (2008) do not include the second term containing the end load. We guessed at the form of this term such that it would provide the thin plate solution for a shell with dimensions much greater than the buckling wavelength. We test this addition below and show it gives the correct asymptotic behavior.

The differential equation is solved by expanding the vertical deformation w and initial load q in terms of Legendre polynomials

$$w(\theta) = \sum_{l=2}^{\infty} W_l P_l(\theta) \quad (17)$$

Note that the Laplacian operator applied to a Legendre polynomial is $-l(l+1)$. After this substitution the differential equation (Eq. (14)) becomes

$$\begin{aligned} \eta D [-l(l+1)][2-l(l+1)][2-l(l+1)] W_l + FR^2 [2-l(l+1)][2-l(l+1)] W_l + EhR^2 [2-l(l+1)] W_l + R^4 (1-\nu-l(l+1)) \Delta\rho g W_l \\ = R^4 (1-\nu-l(l+1)) q_o \end{aligned} \quad (18)$$

After a little algebra, we arrive at an equation for the deflection of the shell that is similar to the flat-Earth equation

$$W_l = q_o \left[\frac{\eta D \frac{l(l+1)[l(l+1)-2][l(l+1)-2]}{R^4 [l(l+1)-1+\nu]} - \frac{F}{R^2} \frac{[l(l+1)-2][l(l+1)-2]}{[l(l+1)-1+\nu]} + \frac{Eh}{R^2} \frac{[l(l+1)-2]}{[l(l+1)-1+\nu]} + \Delta\rho g \right]^{-1} \quad (19)$$

We can check that this is the appropriate equation by taking the limit as $h/R \rightarrow 0$. We can approximate $l = 2\pi kR$, where k is the wavenumber. Note that η goes to 1 and the third term in brackets goes to zero. For large l , all the terms in square brackets reduce to $(2\pi kR)^2$. The equation becomes

$$W_l = q_o [D(2\pi k)^4 - F(2\pi k)^2 + \Delta\rho g]^{-1} \quad (20)$$

which is equivalent to the thin plate solution.

The denominator of the spherical flexure equation should be analyzed to determine the critical end load and the harmonic degree of buckling. We will first explore these functions under conditions appropriate to buckling on the Earth where the wavelength is small compared with the radius of the Earth. We will then use parameters appropriate for Iapetus and restrict the buckling wavelength to even harmonics because we expect the solutions to be symmetric about the equator.

The denominator of the spherical and Cartesian flexure equations is shown in Fig. 2. The parameter values are appropriate for the Earth with $R = 6371$ km, $\rho_o = 5500$ kg m⁻³, $h = 50$ km, $E = 6.5 \times 10^{10}$ Pa and $\nu = 0.25$. In this case, the critical end load and average end stress are 3.9×10^{14} N m⁻¹ and 7.8×10^9 Pa, respectively. The lithosphere buckles at a wavelength of 380 km corresponding to a spherical harmonic degree of 105. The lower plot in Fig. 2 shows

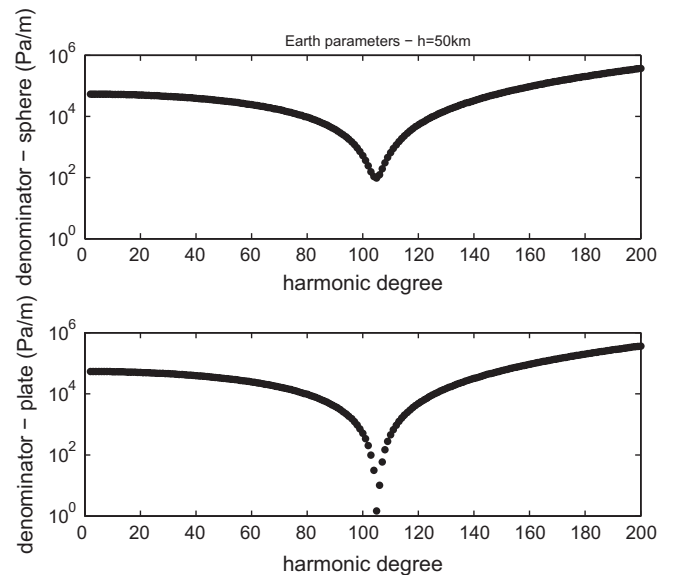


Fig. 2. Denominators of Eqs. (19) (upper) and (20) (lower) showing the buckling singularity for the approximate conditions found in the Earth’s oceanic lithosphere. In both cases the strength of the singularity can be increased by increasing the end load.

the thin plate solution where the denominator goes exactly to zero at the buckling wavelength. The upper plot shows the thin shell with the same behavior, but the singularity is not as strong. Of course, in the real world non-linear processes will dominate long before the conditions become exactly singular (McAdoo and Sandwell, 1985). The upper part of the shell will undergo brittle faulting (Beeman et al., 1988) while the lower part of the shell may undergo ductile deformation according to power-law rheology (Goldsby and Kohlstedt, 2001).

Next, we apply this analysis to the case of Iapetus $R = 730$ km, $\rho_0 = 1000 \text{ kg m}^{-3}$, $h = 60, 80, 100,$ and 120 km, $E = 9 \times 10^9$ Pa and $\nu = 0.35$ (Fig. 3). (A lower value of $E = 4.5 \times 10^9$ Pa is also considered.) In this case the buckling singularity occurs at a low spherical harmonic degree, so the spherical equations are used. Because of symmetry, the deformation must occur at the even harmonic degrees 2, 4, 6, ... For Iapetus the main unknown parameter is the shell thickness. Our proposal for the formation of the equatorial ridge and excess flattening requires that the shell maintain its pre-deformation radius, so the buckling/flexural wavelength must be concentrated at degree 2. This seems to require that the shell thickness exceeds about 120 km. This value is realistic based on previous analyses of the topography of Iapetus (Giese et al., 2008) wherein an elastic thickness greater than 50–100 km is required to maintain the elevated topography of the equatorial ridge.

Based on our analysis, we find that degree-2 buckling is possible; however, as expected based on the Earth calculations, we also find that the end load needed to buckle the 120 km-thick shell ($3.4 \times 10^{13} \text{ N m}^{-1}$ and 280 MPa) is much larger than the end load available from gravitational contraction (only 12 MPa). As on the Earth, these end loads cannot exceed the integrated yield strength of the lithosphere. The strongest possible lithosphere on Iapetus would consist of a fully brittle layer over a ductile core whose strength is governed by Byerlee's law for ice (Beeman et al., 1988). In this case the maximum depth-averaged strength would be $\bar{\sigma} = 0.69\rho gh/2$ or 8.3 MPa. A more realistic triangular yield strength envelope would have an average strength of 4.1 MPa. So,

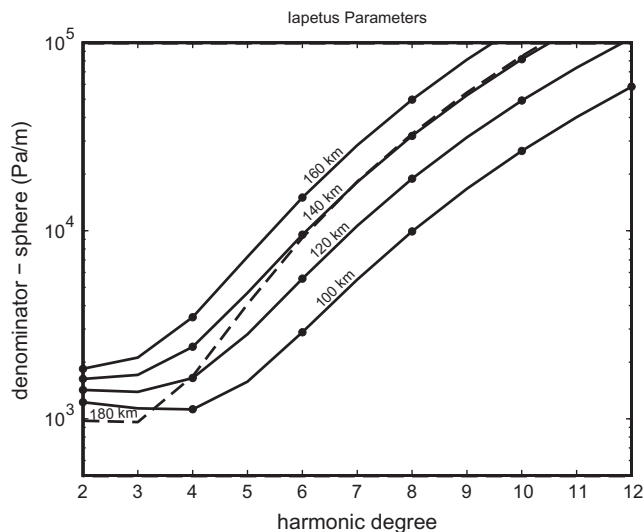


Fig. 3. Denominator of the spherical shell flexure equation using parameters appropriate to Iapetus. The solution for the 60-km thick plate has a pronounced singularity at spherical harmonic degree 6. This singularity becomes weaker and broader as the shell thickness increases. For thicknesses greater than 100 km, degree 2 becomes the dominant buckling mode. The dashed curve is for a 2 times lower Young's modulus. For this case a thickness greater than 180 km is needed to have degree-2 dominate. This analysis also illustrates that a thickness >120 km is needed to keep the collapsing hemispheres from flexurally deforming toward a more spherical isostatic equilibrium associated with the present 79 days rotation rate.

as was found for the Earth's lithosphere, the elastic buckling stress (280 MPa) is much greater than the gravitational contraction stress (12 MPa), which is somewhat greater than the average strength of the lithosphere (4–8 MPa). These calculations show that lithospheric deformation on Iapetus is possible and that an initial perturbation could begin as a degree-2 deformation, although this pattern would quickly become focused at smaller scales on folds and faults just as it does in the Indian Ocean on the Earth, where deformation became focused along the fossil spreading ridges and fracture zones.

Both the magnitude and orientation of the stress tensor will affect the style of faulting in a spherical shell (Melosh and Dzurisin, 1978). Despinning of a planet consisting of a thin shell over a fluid mantle, initially in hydrostatic equilibrium, will result in a stress field that has E–W compression and N–S tension at the equator and general extension at the polar regions. According to the Anderson theory of faulting, this will result in strike-slip faults focused in equatorial regions (Melosh and Dzurisin, 1978). A degree-2 buckling will produce a stress field that is similar to spinning up a planet. In addition there will be a uniform contraction stress that is driving the buckling. If the spin-up stress is equal to (or less than) the contraction stress, then the combination will have large N–S compression at the equator and zero stress (or slightly compressional) E–W as shown in Fig. 4. Near the poles both stress components will be compressional and generally larger than the equatorial stress. A focusing of the stress along the equator, which is needed to form an equatorial ridge, may require a 2 times thinner lithosphere along the equator, as proposed by Beuthe (2009). A better understanding of what is required to focus the deformation along an equatorial ridge is beyond the scope of this study. It will require a finite-element type of model including a finite yield strength brittle upper lithosphere (Beeman et al., 1988) and a ductile lower lithosphere having a power-law rheology (Goldsby and Kohlstedt, 2001).

2.3. Change in surface area, removal of equatorial ring, and final shape

The last issue considered here is whether the gravitational collapse model, with equatorial strain concentration, is geometrically consistent with the observations. Assuming the average density of Iapetus increases by 10%, then the volume must decrease by 10%. First we calculate the reduction in radius, then the reduction in area, and finally remove the area from an equatorial band. The change in radius is given by

$$r_f = r_0 \left(\frac{V_f}{V_0} \right)^{1/3} \quad (21)$$

where V_0 , V_f , r_0 , and r_f are the initial volume, final volume, initial radius, and final radius, respectively. The change in area is given by

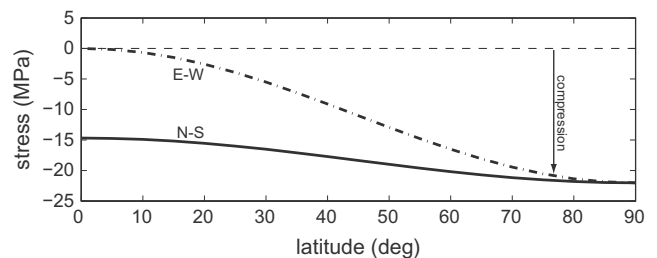


Fig. 4. North-south and east-west stress components associated with a contraction and deformation from degree-2 buckling. The radial stress component for a thin shell is zero. The magnitude of the degree-2 stress must be less than or equal to the compressive stress to promote E–W oriented thrust faults in the equatorial region. In other words the sigma-1 stress must be vertical and sigma-3 stress must be N–S to obtain thrust faults.

$$\Delta A = -4\pi r_0^2 \left[1 - \left(\frac{V_f}{V_0} \right)^{2/3} \right] \quad (22)$$

For a volume change of 10%, the corresponding decrease in area with respect to the present area is 7%.

The main issue is how this area is removed. Based on the linear stability analysis above, we find that the initial oblate ellipsoidal shape of the moon will be amplified due to the compressional forces on the asymmetric shell. Suppose there is a non-linear strain concentration along the equator creating a triangular ridge ~18 km tall and ~200 km across. Next, suppose that the remainder of the shell remains largely undeformed. We could model the change in shape of the moon by removing the area in an equatorial ring around the equator. The half-height of the ring is equal to the change in half-area divided by the circumference of the moon or

$$\Delta h = r_0 \left[1 - \left(\frac{V_f}{V_0} \right)^{2/3} \right] \quad (23)$$

For a 10% volume reduction and present-day average radius of 735 km, the 1/2 height of the ring removed is 50 km. The shape of the moon will be that of a sphere with an annulus removed. This corresponds to a spherical cap with the origin displaced along the spin axis by an amount Δh as shown in Fig. 5.

We compute the radius of a sphere that is displaced from the origin and compare this with the shape of an ellipsoid. Using the law of cosines, we see

$$r_0^2 = r^2 + \Delta h^2 - 2r\Delta h \cos \left(\theta + \frac{\pi}{2} \right) \quad (24)$$

After a little algebra one arrives at a transcendental equation for the radius as a function of latitude that can be solved by iteration

$$r_{i+1}^2 = r_0^2 - \Delta h^2 - 2\Delta h r_i \sin \theta \quad (25)$$

The shape of Iapetus has been modeled as an ellipsoid of revolution with a polar radius $c = 712$ km and an equatorial radius $a = 747$ km (Thomas et al., 2007). Given that the equatorial ridge obscures part of the elliptical shape of the moon (~10°), is it possible that the actual shape of Iapetus is a sphere with an equatorial ring removed? Fig. 6 shows a comparison between the radius of Iapetus using a displaced sphere (dots) and the best fitting ellipsoid model (solid). The rms difference between the two models is 1.8 km. (Note that a 20° equatorial band of topography has been excluded from the fit because this zone is covered by the equatorial ridge.) The rms fit of the Iapetus shape data to the ellipsoidal model is 3.7 km (Thomas et al., 2007), so the fit of the displaced sphere model is well within this error bound. This best fit model has a Δh of 46 km, which is slightly less than the 50 km estimate related

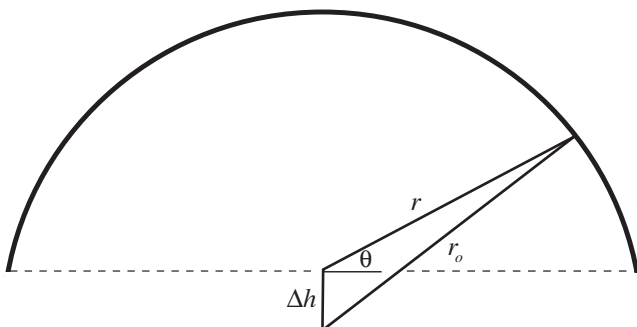


Fig. 5. Diagram showing the radius versus latitude for a spherical cap having an origin displaced along the z-axis by an amount Δh .

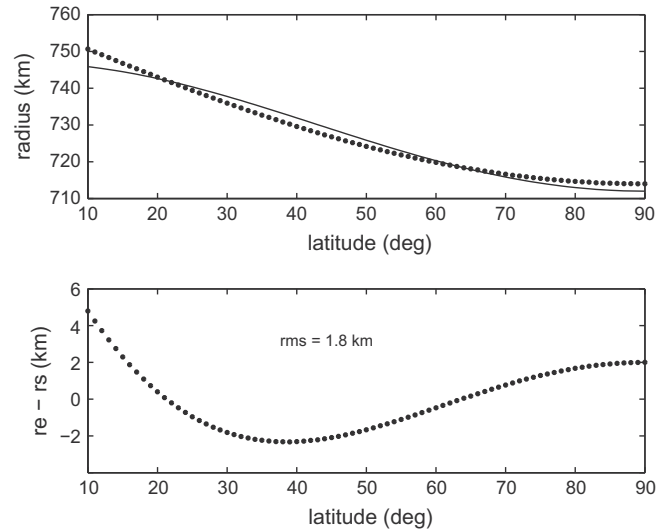


Fig. 6. (Upper) Comparison between the shape of an ellipsoidal model (solid curve) for Iapetus $c = 712$ km and $a = 747$ km (Thomas et al., 2007) and a sphere ($r_0 = 760$ km) with the origin displaced by 46 km (dotted curve). (Lower) The difference between the two models has an rms value of 1.8 km. Note that the comparison begins at 10° north which is outside the areas affected by the equatorial ridge.

to the 10% volume shrinkage. A more definitive analysis would require a re-analysis of the original photographic data or access to the already compiled data of Thomas et al. (2007).

3. Summary, discussion and conclusions

Iapetus is a highly flattened object. Its oblateness is generally attributed to a fossil ellipsoidal bulge from an early state of rapid rotation. This interpretation requires that Iapetus has despun to its present slow rotation, and it strongly constrains the thermal-mechanical evolution of the satellite. Superimposed on the large-scale oblateness is an equatorial ridge of order 100 km wide in the latitudinal direction. The equatorial ridge is likely a consequence of the same phenomenon that produced the global oblateness, but this is a problem for the despinning scenario because stresses produced by despinning should lead to compressional features oriented perpendicular to the equator and not along it (Pechmann and Melosh, 1979). In this paper we have suggested an alternative scenario, not involving despinning from a very high rate of ~7 h, that explains both the global flattening and the equatorial ridge.

While the flattened shape of satellites like Iapetus is usually represented by an ellipsoid, it is instead possible to fit the shape by two spherical caps pieced together along their planar surfaces that are parallel to the equatorial plane. This idealized shape would have an equatorial cusp, but the details of Iapetus' shape at the equator are hidden by the equatorial ridge. The spherical cap shape is produced by the removal of a cylindrical band of material from the equatorial region of an initial spherical shape (perhaps slightly flattened by rotation). This happens because of the early stage collapse of a relatively large porosity in the satellite interior that puts the spherical shell lithosphere of the satellite into a compressional state that fails by an unmodeled buckling instability in the equatorial region as the satellite shrinks in compaction. The redistribution of material as a result of shrinkage in part builds the equatorial ridge as well as a large equatorial root.

The above scenario was shown to be feasible since the gravitational end load in the lithosphere is 1.5–3 times greater than the integrated strength of the lithosphere. All that is required is that

Iapetus had an initial porosity of at least about 10% and that the satellite compacted early in its evolution as it warmed to the creep temperature of ice as a result of heating by long-lived radioactivity in the silicate fraction of the moon. Larger initial porosities would facilitate the deformation. The thickness of Iapetus' lithosphere needs to be about 120 km or somewhat larger to maintain its present-day non-hydrostatic shape. The shape of Iapetus can be fit either by an ellipsoid or by spherical caps to within the uncertainties of the topographic data.

It is emphasized that the proposed scenario explains both the large-scale flattening of Iapetus and its equatorial ridge. It also removes the constraints on the thermal history of Iapetus imposed by a despinning event. It cautions that the oblateness of a satellite is not necessarily a reflection of despinning, although Iapetus is unique in having an equatorial ridge as evidence of possible early buckling instability.

Acknowledgments

We thank William McKinnon, the associate editors, and an anonymous reviewer for their critical reviews of this manuscript. This interaction was needed to clarify the presentation and identify future work needed for testing the hypothesis. Mikael Beuthe provided a copy of his fall 2009 AGU presentation, which helped for refining the deformation hypothesis. Gerald Schubert acknowledges support from the NASA Outer Planets Program NNX09AP29G. David Sandwell was partly supported by the NASA Geodetic Imaging Program NNX09AD12G. ConocoPhillips provided travel support.

References

- Beeman, M., Durham, W.B., Kirby, S.H., 1988. Friction of ice. *J. Geophys. Res.* 93, 7625–7633.
- Beuthe, M., 2008. Thin elastic shells with variable thickness for lithospheric flexure of one-plate planets. *Geophys. J. Int.* 172, 817–841. doi:10.1111/j.1365-246X.2007.03671.x.
- Beuthe, M., 2009. East–west faulting and buckling from the contraction of a lithosphere thinner at the equator, with applications to Mercury and Iapetus. *EOS Trans. AGU (Fall Meet. Suppl)* 90 52. Abstract P41A–09.
- Castillo-Rogez, J.C., Matson, D.L., Sotin, C., Johnson, T.V., Lunine, J.J., Thomas, P.C., 2007. Iapetus' geophysics: Rotation rate, shape, and equatorial ridge. *Icarus* 190, 179–202. doi:10.1016/j.icarus.2007.02.018.
- Cruikshank, D.P., Bell, J.F., Gaffey, M.J., Hamilton Brown, R., Howell, R., Beerman, C., Rognstad, M., 1983. The dark side of Iapetus. *Icarus* 53, 90–104. doi:10.1016/0019-1035(83)90023-4.
- Czechowski, L., Leliwa-Kopystyński, J., 2008. The Iapetus's ridge: Possible explanations of its origin. *Adv. Space Res.* 42, 61–69. doi:10.1016/j.asr.2007.08.008.
- Denk, T., Neukum, G., Roatsch, T., Wagner, R.J., Giese, B., Perry, J.E., Helfenstein, P., Turtle, E.P., Porco, C.C., 2008. Iapetus imaging during the targeted flyby of the Cassini spacecraft. *Lunar Planet. Sci.* 36. Abstract #2262.
- Giese, B., Denk, T., Neukum, G., Roatsch, T., Helfenstein, P., Thomas, P.C., Turtle, E.P., McEwen, A., Porco, C.C., 2008. The topography of Iapetus' leading side. *Icarus* 193, 359–371. doi:10.1016/j.icarus.2007.06.005.
- Goldsby, D.L., Kohlstedt, D.L., 2001. Superplastic deformation of ice: Experimental observations. *J. Geophys. Res.* 106, 11017–11030.
- Ip, W.-H., 2006. On a ring origin of the equatorial ridge of Iapetus. *Geophys. Res. Lett.* 33. L16203. doi:10.1029/2005GL025386.
- Matson, D.L., Castillo-Rogez, J.C., Schubert, G., Sotin, C., McKinnon, W.B., 2009. The thermal evolution and internal structure of Saturn's mid-sized icy satellites. In: Dougherty, M.K., Esposito, L.W., Krimigis, S.M. (Eds.), *Saturn from Cassini-Huygens*. Springer, Netherlands, pp. 577–612. doi:10.1007/978-1-4020-9217-6_18.
- McAdoo, D.C., Sandwell, D.T., 1985. Folding of oceanic lithosphere. *J. Geophys. Res.* 90, 8563–8569.
- McNutt, M.K., Menard, H.W., 1982. Constraints on yield strength in the oceanic lithosphere derived from observations of flexure. *Geophys. J. R. Astron. Soc.* 71, 363–394. doi:10.1111/j.1365-246X.1982.tb05994.x.
- Melosh, H.J., Dzurisin, D., 1978. Mercurian global tectonics: A consequence of tidal despinning? *Icarus* 35, 227–236.
- Melosh, H.J., Nimmo, F., 2009. An intrusive dike origin for Iapetus' enigmatic ridge? *Lunar Planet. Sci.* 40. Abstract #2478.
- Pechmann, J.B., Melosh, H.J., 1979. Global fracture patterns of a despun planet: Application to Mercury. *Icarus* 38, 243–250. doi:10.1016/0019-1035(79)90181-7.
- Porco, C.C., and 34 colleagues, 2005. Cassini imaging science: Initial results on Phoebe and Iapetus. *Science* 307, 1237–1242. doi:10.1126/science.1107981.
- Roberts, J.H., Nimmo, F., 2009. Tidal dissipation due to despinning and the equatorial ridge on Iapetus. *Lunar Planet. Sci.* 40. Abstract #1927.
- Thomas, P.C., and 12 colleagues, 2007. Shapes of the saturnian icy satellites and their significance. *Icarus* 190, 573–584. doi:10.1016/j.icarus.2007.03.012.